

Isomeric Cyclopropenes Exhibit Unique Bioorthogonal Reactivities

David N. Kamber,[†] Lidia A. Nazarova,[†] Yong Liang,[‡] Steven A. Lopez,[‡] David M. Patterson,[†] Hui-Wen Shih,[†] K. N. Houk,^{*,‡,§} and Jennifer A. Prescher^{*,†,‡,§}

Departments of [†]Chemistry, [‡]Molecular Biology & Biochemistry, and [§]Pharmaceutical Science, University of California, Irvine, California 92697, United States

[‡]Department of Chemistry and Biochemistry, University of California, Los Angeles, California 90095, United States

Supporting Information

ABSTRACT: Bioorthogonal chemistries have provided tremendous insight into biomolecule structure and function. However, many popular bioorthogonal transformations are incompatible with one another, limiting their utility for studies of multiple biomolecules in tandem. We identified two reactions that can be used concurrently to tag biomolecules in complex environments: the inverse electron-demand Diels–Alder reaction of tetrazines with 1,3-disubstituted cyclopropenes, and the 1,3-dipolar cycloaddition of nitrile imines with 3,3-disubstituted cyclopropenes. Remarkably, the cyclopropenes used in these transformations differ by the placement of a single methyl group. Such orthogonally reactive scaffolds will bolster efforts to monitor multicomponent processes in cells and organisms.

The bioorthogonal chemical reporter strategy has been widely used to interrogate glycans and other biopolymers in living systems.^{1–5} This approach relies on the introduction of a uniquely reactive functional group (i.e., a “chemical reporter”) into a biomolecule of interest. The chemical reporter can be ligated to probes for visualization or retrieval using highly selective (i.e., “bioorthogonal”) chemistries.^{2,6} While powerful, this two-step strategy has been largely limited to examining one biological feature at a time in live cells and tissues. This is because many bioorthogonal reactions are incompatible with one another and cannot be used in tandem to monitor multiple species.^{7–12}

Our long-term goal is to identify transformations that can be used concurrently to tag biomolecules in complex environments. As a starting point, we were drawn to the cycloaddition reactions of cyclopropenes. Functionalized cyclopropenes are stable in physiological environments, yet readily reactive with dienes and other biocompatible motifs.^{13–17} We and others have shown that 1,3-disubstituted cyclopropenes can be metabolically incorporated into cellular glycans and selectively ligated via inverse electron-demand Diels–Alder (IED-DA) reactions with tetrazines (Figure 1, top).^{14,15,18} In related work, Lin and colleagues demonstrated that 3,3-disubstituted cyclopropenes can be introduced into proteins and ultimately detected via 1,3-dipolar cycloaddition with nitrile imines (Figure 1, bottom).¹⁶ This reaction, similar to the cyclopropene–tetrazine ligation, proceeds readily in cellular environments.

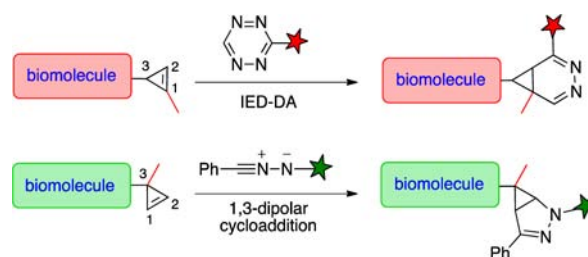


Figure 1. Cyclopropene scaffolds undergo bioorthogonal cycloadditions. 1,3-Disubstituted cyclopropenes (top) react with tetrazines. 3,3-Disubstituted scaffolds (bottom) react with 1,3-dipoles to afford covalent adducts.

We were intrigued by cyclopropene IED-DA and dipolar cycloadditions for an additional reason: these reactions had the potential to be orthogonal to one another and, thus, applicable to multicomponent biomolecule labeling. In earlier work, we observed that 1,3-disubstituted cyclopropenes react with tetrazines at the less-hindered face of the three-membered ring (i.e., the side bearing the C-3 H atom).¹⁴ Additional steric bulk at this position (as in the case of 3,3-disubstituted cyclopropenes) would, in theory, impede IED-DA reactivity but not impact cycloadditions with less sterically encumbered reactants (e.g., 1,3-dipoles).

To predict whether cyclopropene reactivity could be tuned with steric modifications at C-3, we examined the reactions of 1,3- and 3,3-dimethylcyclopropene (Cp(1,3) and Cp(3,3)) with diphenyl-substituted nitrile imine (NI) and tetrazine (Tz) using density functional theory (DFT) calculations.¹⁹ M06-2X,^{20,21} a density functional that provides relatively accurate energetics for cycloadditions,^{22,23} was used to generate the transition-state structures shown in Figure 2. We also analyzed activation barriers using the distortion/interaction model,^{24,25} in which the activation energy (E_{act}) is analyzed in terms of the distortion energy (E_{dist}) required for the reactants to achieve their transition-state geometries, and the interaction energy (E_{int}) arising from orbital overlap between the two distorted reactants in the transition state. The computed activation free energies in water (G_{water}), relative rate constants (k_{rel}), and distortion/interaction energies are provided in Figure 2.

Our calculations indicate that for the sterically less encumbered nitrile imine, 1,3-dimethylcyclopropene reacts

Received: August 2, 2013

Published: September 3, 2013

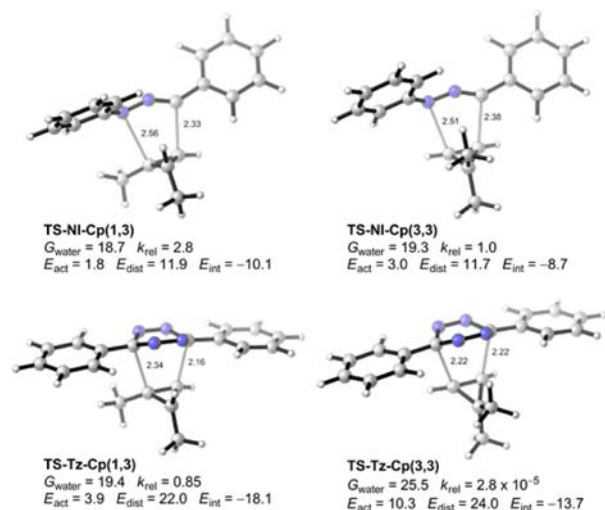


Figure 2. M06-2X/6-31G(d)-optimized transition-state structures for the cycloadditions of 1,3- and 3,3-dimethylcyclopropene [Cp(1,3) and Cp(3,3)] with diphenyl-substituted nitrile imine (NI) and tetrazine (Tz). M06-2X/6-311+G(d,p)//6-31G(d)-computed energies and relative rate constants (distances in Å, energies in kcal/mol, k_{rel} based on G_{water} at 298 K) are also shown.

only 2.8 times faster than 3,3-dimethylcyclopropene. The distortion and interaction energies are very close, suggesting that increased steric bulk at C-3 of the cyclopropene does not dramatically influence reactivity with linear 1,3-dipoles. However, placement of a single methyl group at C-3 reduces cyclopropene reactivity by over 4 orders of magnitude in the IED-DA reaction. In the transition state **TS-Tz-Cp(3,3)**, to avoid steric clashes between the C-3 methyl and tetrazine nitrogens, the dihedral angle between the cyclopropene plane and the C–C bonds-forming plane increases to 120° , about 15° larger than the corresponding value in **TS-Tz-Cp(1,3)**. In Figure 2, note how the cyclopropene C-3 and methyl groups are tilted away from the tetrazine. This results in increased distortion energy (24.0 versus 22.0 kcal/mol) and less favorable interaction energy (-13.7 versus -18.1 kcal/mol) due to poorer orbital overlap. Similar reactivities were predicted for more functionalized cyclopropenes and tetrazines (Figure S1). Collectively, these data suggest that isomeric cyclopropenes possess unique bioorthogonal reactivities: 3,3-disubstituted cyclopropenes should react readily with nitrile imines, but not tetrazines, under physiological conditions; 1,3-disubstituted cyclopropenes, by contrast, should react readily with both.

To test these predictions, we synthesized a panel of disubstituted cyclopropenes bearing methyl groups at either C-1 or C-3. The scaffolds also comprise amide or carbamate groups as these linkages mimic those found in numerous bioconjugates. The amide-functionalized probes **1a,b** were synthesized similarly to previous reports (Scheme 1).^{14–16} In brief, esters **3a,b** were subjected to base-catalyzed hydrolysis. The resulting acids (**4a,b**) were subsequently treated with PFP-TFA, followed by isopropylamine to access the desired probes. To prepare the carbamate scaffolds, esters **3a,b** were first reduced with DIBAL-H. The reaction with **3b** was prone to cyclopropane formation; over-reduction was avoided at -78°C . Alcohols **5a,b** were ultimately converted to the desired carbamates (**2a,b**) via CDI coupling with isopropylamine, followed by TMS removal.

Scheme 1. Synthesis of Disubstituted Cyclopropenes

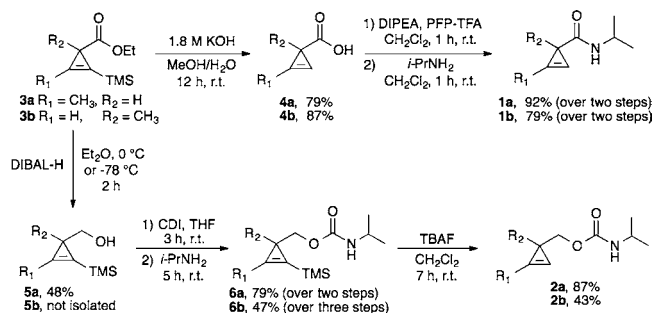


Table 1. Second-Order Rate Constants for the Cyclopropene–Tetrazine Ligation

Cyclopropene	Tetrazine	k_2 ($\times 10^{-2} \text{ M}^{-1} \text{ s}^{-1}$)
1a	7	3.19 ± 0.45
1b	7	N/R*
1b	8	N/R*
2a	7	277.8 ± 36.6
2b	7	N/R*
2b	8	N/R*

All rate constants were measured in 15% DMSO/PBS. N/R indicates no reaction observed after 90 min.

With the desired cyclopropenes in hand, we analyzed their reactivity with model tetrazines (Table 1). Tetrazines **7** and **8** were incubated with excess cyclopropene, and the cycloadditions were monitored by the change in tetrazine absorbance over time. As shown in Figures 3 and S2, robust IED-DA reactivity was observed with the 1,3-disubstituted scaffolds **1a** and **2a**, while no reactivity was detected with their 3,3-disubstituted counterparts (**1b** and **2b**). In fact, no reaction between **1b** or **2b** and tetrazine **7** was observed in phosphate buffer even after 24 h at elevated temperature (Figure S3).

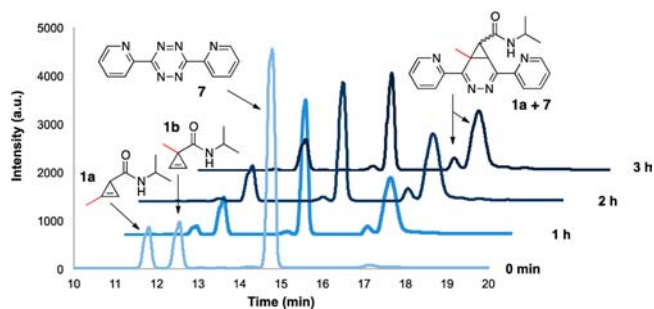
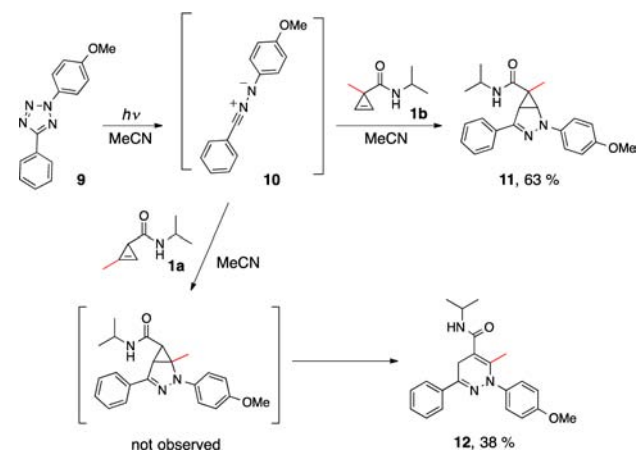


Figure 3. Tetrazines react selectively with 1,3-disubstituted cyclopropenes. Cyclopropenes **1a,b** (5 mM in 15% MeCN/PBS) were treated with tetrazine **7** (10 mM) and monitored by HPLC. The initial cycloadduct formed between **1a** and **7** can undergo further intramolecular cyclization in aqueous solution.¹⁴

Minimal IED-DA reactivity with the 3,3-disubstituted probes was observed only in the presence of large amounts of organic solvent, and in these cases, the transformations were quite slow (Table S2). It should also be noted that the tetrazine–cyclopropene ligations revealed the expected trends, with the more electron-rich carbamates and less sterically hindered tetrazine exhibiting the fastest rates (Table 1).^{26,27}

Despite their extremely sluggish reaction kinetics with tetrazines, 3,3-disubstituted cyclopropenes react readily with nitrile imines in “photo-click” reactions.¹⁶ Indeed, when micromolar concentrations of **1b** and **9** were subjected to UV light (generating **10** *in situ*), the fluorescent cycloadduct **11** was formed in less than 5 min (Scheme 2). The corresponding 1,3-

Scheme 2. Cyclopropenes React with Nitrile Imines To Generate Stable Cycloadducts



cyclopropene **1a** also reacted rapidly with **10** to provide the rearranged cycloadduct **12**. Similar rearrangements have been observed in cycloadditions with cyclopropenes and nitrile oxides.²⁸ Both ligation products **11** and **12** were found to be stable in aqueous solution for over three days. Importantly, nitrile imine **10** could also be generated in the presence of tetrazine **7** with no observable side reactivity, highlighting the compatibility of these reagents (Figure S4).

The unique reactivity profiles of 1,3- and 3,3-disubstituted cyclopropenes suggested that the probes could be used in tandem for biomolecule labeling. To test this hypothesis, we functionalized model proteins (BSA and lysozyme) with the isomeric cyclopropenes **13a,b** using standard coupling conditions (Figure 4A). Mass spectrometry analysis was used to verify that equivalent numbers of cyclopropenes were appended to the biomolecules (Figure S5). When the proteins were treated with a tetrazine–rhodamine conjugate (**Tz-Rho**), only samples functionalized with 1,3-disubstituted cyclopropenes (**Cp(1,3)**) showed robust dose- and time-dependent labeling, in agreement with our kinetic data (Figures 4B, S6, and S7). No labeling above background was observed with proteins outfitted with 3,3-disubstituted cyclopropenes (**Cp(3,3)**). Both **Cp(1,3)** and **Cp(3,3)** samples were covalently modified with nitrile imines using “photo-click” conditions (Figures 4C and S7). The fluorescent intensities of the **Cp(1,3)** adducts were somewhat reduced, though, likely due to the decreased absorption efficiency of the products (**12** versus **11**, Figure S8). When conjugates **Cp(1,3)** and **Cp(3,3)** were subjected to both cycloaddition reactions (treatment with **Tz-Rho**, followed by **9**), tetrazine labeling was again only observed for **Cp(1,3)**

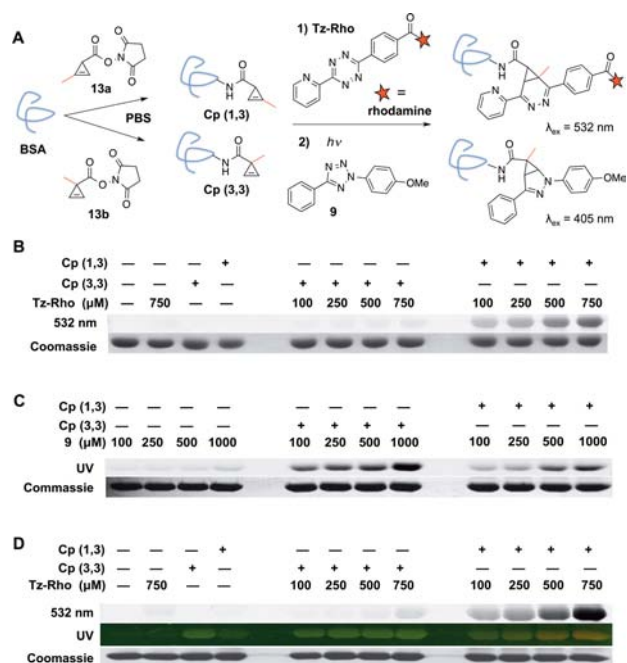


Figure 4. Cyclopropenes can be selectively detected on model proteins. (A) Cyclopropenes **13a,b** were appended to BSA. The modified proteins **Cp(1,3)** and **Cp(3,3)** were subsequently reacted with either a tetrazine–rhodamine conjugate (**Tz-Rho**) or nitrile imine **10** (generated via photolysis of **9**). (B) Gel analysis of **Cp(1,3)** or **Cp(3,3)** incubated with **Tz-Rho** (100–750 μ M) or no reagent (—) for 1 h. (C) Gel analysis of **Cp(1,3)** or **Cp(3,3)** treated with **9** (100–1000 μ M) and UV irradiation. (D) Analysis of samples treated with **Tz-Rho** (100–750 μ M) or no reagent (—), followed by **9** (5 mM) and UV irradiation (in gel). The gel was scanned at 532 nm (top) to visualize rhodamine, and also illuminated with UV light (middle) to visualize nitrile imine cycloadducts (green). The red color in the UV-illuminated gel (middle) is due to rhodamine fluorescence. For B–D, protein loading was assessed with Coomassie stain.

samples. The **Cp(3,3)** samples, along with unmodified scaffolds on **Cp(1,3)**, were detected following nitrile imine generation (Figures 4D and S7).

In sum, we have identified cyclopropenes that exhibit unique modes of bioorthogonal reactivity. Computational analyses predicted that 1,3-disubstituted cyclopropenes would undergo facile IED-DA reactions, while 3,3-disubstituted scaffolds would be minimally reactive with tetrazines. Upon synthesis and *in vitro* characterization of a panel of modified cyclopropenes, we discovered that scaffolds that differ in the placement of a single methyl group (C-1 vs C-3) exhibit vastly different IED-DA reaction profiles: 1-methylcyclopropenes can be selectively ligated with tetrazine probes in the presence of 3-methylcyclopropenes; the unmodified 3-methyl-substituted scaffolds can be efficiently ligated via dipolar cycloaddition. The ability to selectively modify isomeric cyclopropenes—and ultimately target them to discrete biomolecules—will facilitate multicomponent imaging studies *in vitro* and in live cells. The cyclopropene scaffold also offers unique opportunities for further biocompatible reaction development, including selective nucleophilic additions and normal-demand Diels–Alder reactions. An arsenal of such orthogonal reactions will continue to provide insight into complex biological systems.^{29,30}

■ ASSOCIATED CONTENT

■ Supporting Information

Experimental details, full spectroscopic data for all new compounds, and additional computational data. This material is available free of charge via the Internet at <http://pubs.acs.org>.

■ AUTHOR INFORMATION

Corresponding Authors

houk@chem.ucla.edu

jpresche@uci.edu

Notes

The authors declare no competing financial interest.

■ ACKNOWLEDGMENTS

This work was supported by the UCI School of Physical Sciences and the NSF (CHE-1059084). Calculations were performed on the Hoffman2 cluster at UCLA and the Extreme Science and Engineering Discovery Environment (XSEDE), which is supported by the NSF (OCI-1053575). We thank members of the UCI Chemistry Department for providing reagents and equipment. We also thank Drs. John Greaves and Beniam Berhane for assistance with mass spec analyses.

■ REFERENCES

- (1) Chang, P. V.; Prescher, J. A.; Hangauer, M. J.; Bertozzi, C. R. *J. Am. Chem. Soc.* **2007**, *129*, 8400.
- (2) Prescher, J. A.; Bertozzi, C. R. *Nat. Chem. Biol.* **2005**, *1*, 13.
- (3) Prescher, J. A.; Dube, D. H.; Bertozzi, C. R. *Nature* **2004**, *430*, 873.
- (4) Hang, H. C.; Wilson, J. P.; Charron, G. *Acc. Chem. Res.* **2011**, *44*, 699.
- (5) Haun, J. B.; Devaraj, N. K.; Hilderbrand, S. A.; Lee, H.; Weissleder, R. *Nat. Nanotechnol.* **2010**, *5*, 660.
- (6) Sletten, E. M.; Bertozzi, C. R. *Angew. Chem., Int. Ed.* **2009**, *48*, 6974.
- (7) Debets, M. F.; van Berkel, S. S.; Dommerholt, J.; Dirks, A. J.; Rutjes, F. P. J. T.; van Delft, F. L. *Acc. Chem. Res.* **2011**, *44*, 805.
- (8) Lang, K.; Davis, L.; Wallace, S.; Mahesh, M.; Cox, D. J.; Blackman, M. L.; Fox, J. M.; Chin, J. W. *J. Am. Chem. Soc.* **2012**, *134*, 10317.
- (9) Chen, W.; Wang, D.; Dai, C.; Hamelberg, D.; Wang, B. *Chem. Commun.* **2012**, *48*, 1736.
- (10) Plass, T.; Milles, S.; Koehler, C.; Schultz, C.; Lemke, E. A. *Angew. Chem., Int. Ed.* **2011**, *50*, 3878.
- (11) Liang, Y.; Mackey, J. L.; Lopez, S. A.; Liu, F.; Houk, K. N. *J. Am. Chem. Soc.* **2012**, *134*, 17904.
- (12) Sanders, B. C.; Friscourt, F.; Ledin, P. A.; Mbua, N. E.; Arumugam, S.; Guo, J.; Boltje, T. J.; Popik, V. V.; Boons, G. J. *J. Am. Chem. Soc.* **2011**, *133*, 949.
- (13) Zhu, Z.-B.; Wei, Y.; Shi, M. *Chem. Soc. Rev.* **2011**, *40*, 5534.
- (14) Patterson, D. M.; Nazarova, L. A.; Xie, B.; Kamber, D. N.; Prescher, J. A. *J. Am. Chem. Soc.* **2012**, *134*, 18638.
- (15) Yang, J.; Šečková, J.; Cole, C. M.; Devaraj, N. K. *Angew. Chem., Int. Ed.* **2012**, *51*, 7476.
- (16) Yu, Z.; Pan, Y.; Wang, Z.; Wang, J.; Lin, Q. *Angew. Chem., Int. Ed.* **2012**, *51*, 10600.
- (17) Thalhammer, F.; Wallfahner, U.; Sauer, J. *Tetrahedron Lett.* **1990**, *31*, 6851.
- (18) Cole, C. M.; Yang, J.; Šečková, J.; Devaraj, N. K. *ChemBioChem* **2013**, *14*, 205.
- (19) Frisch, M. J.; et al. *Gaussian 09*, revision C.01; Gaussian, Inc.: Wallingford, CT, 2010.
- (20) Zhao, Y.; Truhlar, D. G. *Acc. Chem. Res.* **2008**, *41*, 157.
- (21) Zhao, Y.; Truhlar, D. G. *Theor. Chem. Acc.* **2008**, *120*, 215.
- (22) Lan, Y.; Zou, L.; Cao, Y.; Houk, K. N. *J. Phys. Chem. A* **2011**, *115*, 13906.

- (23) Paton, R. S.; Mackey, J. L.; Kim, W. H.; Lee, J. H.; Danishefsky, S. J.; Houk, K. N. *J. Am. Chem. Soc.* **2010**, *132*, 9335.
- (24) Ess, D. H.; Houk, K. N. *J. Am. Chem. Soc.* **2007**, *129*, 10646.
- (25) Gordon, C. G.; Mackey, J. L.; Jewett, J. C.; Sletten, E. M.; Houk, K. N.; Bertozzi, C. R. *J. Am. Chem. Soc.* **2012**, *134*, 9199.
- (26) Diev, V. V.; Kostikov, R. R.; Gleiter, R.; Molchanov, A. P. *J. Org. Chem.* **2006**, *71*, 4066.
- (27) Karver, M. R.; Weissleder, R.; Hilderbrand, S. A. *Bioconjugate Chem.* **2011**, *22*, 2263.
- (28) Chen, S.; Ren, J.; Wang, Z. *Tetrahedron* **2009**, *65*, 9146.
- (29) Willems, L. I.; Li, N.; Florea, B. I.; Ruben, M.; van der Marel, G. A.; Overkleeft, H. S. *Angew. Chem., Int. Ed.* **2012**, *51*, 4431.
- (30) Sletten, E. M.; Bertozzi, C. R. *J. Am. Chem. Soc.* **2011**, *133*, 17570.